The Co-ordination of Small Molecules by Manganese(II) Phosphine Complexes. Part 14.† Some Novel Mixed Tertiary Phosphine–t-Butyl Isocyanide Complexes of Manganese(II): $[MnBr_2(CNBu^t)(PPhMe_2)]$ and $[Mn(CNBu^t)_4(PR_3)_2]^{2+}$ (PR_3 = $PPhMe_2$, PPh_2Me, $PPhEt_2$, or $PPr^n{}_3$), and the *X*-Ray Crystal Structure of Bis(dimethylphenylphosphine)tetrakis(t-butyl isocyanide)manganese(II) Bis[tribromo(dimethylphenylphosphine oxide)manganate(II)], $[Mn(CNBu^t)_4(PPhMe_2)_2][MnBr_3(OPPhMe_2)]_2$‡

Brian Beagley, Christopher G. Benson, George A. Gott, Charles A. McAuliffe*, Robin G. Pritchard, and S. Peter Tanner
Department of Chemistry, University of Manchester Institute of Science and Technology, P.O. Box 88, Manchester M60 1QD

The complex $[MnBr_2(CNBu^t)(PPhMe_2)]$ has been prepared by reaction of $[MnBr_2(PPhMe_2)]$ with $CNBu^t$. In ethanol solution rearrangement occurs to give the complex $[Mn(CNBu^t)_4(PPhMe_2)_2][MnBr_4]$ and this reacts with other phosphines to yield $[Mn(CNBu^t)_4(PR_3)_2]^{2+}$ (PR_3 = $PPr^n{}_3$, $PPhEt_2$, or PPh_2Me). Air oxidation of an ethanol solution of $[Mn(CNBu^t)_4(PPhMe_2)_2]^{2+}$ produces red crystals of $[Mn(CNBu^t)_4(PPhMe_2)_2][MnBr_3(OPPhMe_2)]_2$ the structure of which is reported. In the cation Mn^{II} is octahedrally co-ordinated and lies on a crystallographic inversion centre. The latter also relates each pair of anions which have Mn^{II} in tetrahedral co-ordination. The Mn–P bonds of the cation are rather short at 2.344(3) Å whereas all other cation and anion dimensions are unremarkable.

The isocyanide ligand in transition-metal complexes can be formally regarded as an analogue of the CO ligand. However, the isocyanide is a stronger σ-donor and a weaker π-acceptor, and as a result the isocyanide ligand can stabilise higher oxidation states.[1] Although isocyanide complexes of Group 6A metals are well documented (see, for example, refs. 2—6), and there has been recent interest in the spectroscopic[7,8] and chemical[6,9—15] properties of homoleptic isocyanide complexes, there are few reports of isocyanide complexes of Group 7A metals, and it is only recently that complexes with Tc have been reported.[16,17]

Manganese forms isocyanide complexes in the 0, +1, +2, and +3 oxidation states during cyclic voltammetry of $[Mn(CNR)_6]^{z+}$ (R = Me or Ph, z = 1, 2, or 3).[18—21] Manganese(II) isocyanide complexes containing $[Mn(CNR)_6]^{2+}$ (*e.g.* R = Ph, Et, Bu^t, or $CH{=}CH_2$)[22] are known,[19,22,23] and are usually prepared *via* the electrolytic or chemical (*e.g.* nitric acid) oxidation of the corresponding manganese(I) complex followed by precipitation with the appropriate anion. In the case of manganese(I) complexes ν(CN) decreases upon co-ordination, indicating d-π^*_{CN} bonding in the complexes, whereas for the corresponding manganese(II) complex ν(CN) increases.[19,24] In contrast to this type of complex, fewer complexes are known which contain both isocyanide and tertiary phosphine ligands.

Here we report the first examples of manganese(II) complexes containing both isocyanide and tertiary phosphine ligands: $[MnBr_2(CNBu^t)(PPhMe_2)]$ and $[Mn(CNBu^t)_4(PR_3)_2]X_2$ {PR_3 = $PPhMe_2$, PPh_2Me, $PPhEt_2$, or $PPr^n{}_3$, X_2 = $[MnBr_4]$ or $[PF_6]_2$}. In addition, the *X*-ray crystal structure of *trans*-$[Mn(CNBu^t)_4(PPhMe_2)_2]^{2+}$, isolated as the $[MnBr_3(OPPhMe_2)]^-$ salt, is reported. Our interest in the manganese(II) phosphine complexes, $[MnBr_2(PR_3)]$, stems from our discovery that these complexes can reversibly co-ordinate small molecules such as dioxygen,[25—27] carbon monoxide,[28] and nitric oxide[29] under very mild conditions and irreversibly co-ordinate sulphur dioxide[30] and carbon disulphide.[31] It was of interest, therefore to investigate systems containing isocyanide ligands.

Results and Discussion

We have determined the structure of the $[MnI_2(PPhMe_2)]$ complex, in which Mn atoms are alternately tetrahedrally (MnI_4) and pseudo-octahedrally (MnI_4P_2) co-ordinated, with the Mn–I–Mn bridged chains extending throughout the crystal, (I).[32] We postulate that small molecules (O_2, CO, and NO) co-ordinate at the co-ordinatively unsaturated (MnX_4) sites and have shown that it is possible to add PR_3 ligands to $[MnX_2(PR_3)]_n$ species to form monomeric pseudo-tetrahedral $[MnX_2(PR_3)_2]$ species.[33] Recently Wilkinson and co-workers[34] and Kohler and co-workers[35] have isolated and structurally characterised monomeric bis(phosphine) $[MnX_2(PR_3)_2]$ complexes. We thus decided to add t-butyl isocyanide to $[MnX_2(PR_3)]$ species in non-co-ordinating solvents in order to produce the isocyanide adducts, $[MnX_2(CNR)(PR_3)]$.

$[MnBr_2(CNBu^t)(PPhMe_2)]$.—This deep blue complex, Table 1, was initially prepared by treating $[MnBr_2(PPhMe_2)]$ with a stoicheiometric quantity of $CNBu^t$ in toluene under strictly anhydrous conditions under argon. Surprisingly, we subsequently discovered that this complex could be prepared by mixing stoicheiometric quantities of anhydrous $MnBr_2$, $PPhMe_2$, and $CNBu^t$ in toluene (see Scheme). Whichever route is used the properties of the resulting complex, $[MnBr_2(CNBu^t)(PPhMe_2)]$, are identical. The complex exhibits a strong i.r. absorption at 2 135 cm^{-1} (Table 1) assignable to ν(CN) of co-ordinated $CNBu^t$; this band is shifted to higher energy from that of free $CNBu^t$, 2 122 cm^{-1}, and suggests that the Mn–C bond is predominantly of σ character, as expected for metals in normal or higher oxidation states.[19,24,34—37] The far-i.r. spectrum

---

† For Part 13 see ref. 27.

‡ *Supplementary data available:* see Instructions for Authors, *J. Chem. Soc., Dalton Trans.*, 1988, Issue 1, pp. xvii—xx.

Non-S.I. unit employed: G = 10^{-4} T.

Table 1. Elemental analyses* and infrared data for the complexes

Complex	Colour	Analysis (%) C	H	N	P	I.r./cm^{-1} ν(CN)	Far-i.r./cm^{-1} ν(P–F)	ν(Mn–Br)	ν(Mn–C)
$[MnBr_2(CNBu^t)(PPhMe_2)]$	Deep blue	35.4 (35.8)	5.2 (4.6)	3.6 (3.2)	6.5 (7.1)	2 135s		194s	220s
$[Mn(CNBu^t)_4(PPhMe_2)_2][MnBr_4]$	Red	41.3 (41.6)	5.5 (5.6)	5.2 (5.4)	6.0 (6.0)	2 140s		230m	314s
$[Mn(CNBu^t)_4(PPhMe_2)_2][PF_6]_2$	Pink	45.0 (45.3)	6.2 (6.1)	5.9 (5.9)	12.8 (13.0)	2 140s	838s		313s
$[Mn(CNBu^t)_4(PPh_2Me)_2][PF_6]_2$	Pink	49.2 (51.2)	5.9 (5.8)	5.6 (5.2)	11.0 (11.5)	2 138s	842s		309s
$[Mn(CNBu^t)_4(PPhEt_2)_2][PF_6]_2$	Pink	46.6 (47.5)	6.5 (6.5)	4.0 (5.5)	12.1 (12.3)	2 142s	840s		315s
$[Mn(CNBu^t)_4(PPr^n_3)_2][PF_6]_2$	Pink	48.4 (45.7)	8.6 (7.8)	5.0 (5.6)	11.3 (12.4)	2 138s	840s		310s

* Calculated values in parentheses.

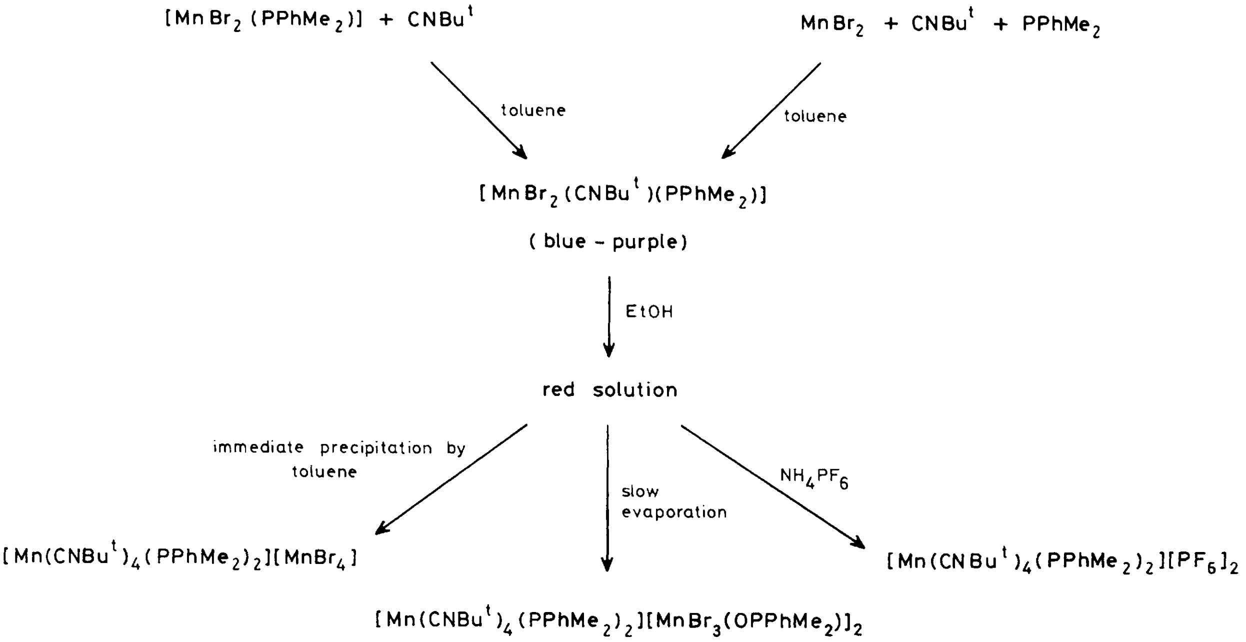

Scheme.

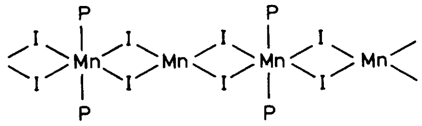

(I)

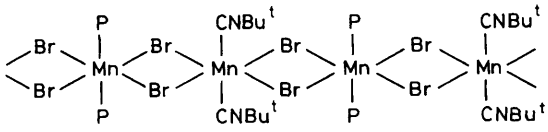

(II)

exhibits a band at 194 cm^{-1} assignable to ν(Mn–Br) of the Mn–Br–Mn linkage {this band is little shifted from that of $[MnBr_2(PPhMe_2)]$, 197 cm^{-1}}, and a band at 220 cm^{-1} is assigned to ν(Mn–C).

Since the ν(Mn–Br–Mn) bands in $[MnBr_2(PPhMe_2)]$ and $[MnBr_2(CNBu^t)(PPhMe_2)]$ are almost identical this strongly suggests that the polymeric structure, (**I**), is retained upon binding of the CNBu^t moiety, to give (**II**). The deep blue colour of (**II**) is, however, somewhat puzzling. Reaction of $[MnX_2(PR_3)]$ with small molecules fall into two broad categories, *viz.* oxidising ligands such as dioxygen,[25–27] nitric oxide,[29] and tetracyanoethylene[38] form deeply coloured Mn^{III}–L$^-$ species (L = small molecule), whereas 'innocent' non-oxidising adduct molecules such as sulphur dioxide,[30] carbon monoxide,[28] or carbon disulphide[31] form only pale coloured Mn^{II}–L species, little different in colour from the original $[MnX_2(PR_3)]$ complex. However, all the available evidence points to the fact that in $[MnBr_2(CNBu^t)(PPhMe_2)]$ manganese is in the +2 oxidation state. The room temperature magnetic moment, 5.2 μ_B, is not indicative of a manganese(III) complex, but is consistent with manganese(II) centres somewhat antiferromagnetically coupled as in (**II**). The room-temperature solid-state e.s.r. spectrum exhibits only a single intense peak at $g = 2$, which, while yielding no structural information, does point to manganese in the +2 oxidation state. Figure 1 shows the solid visible reflectance spectra of $[MnBr_2(CNBu^t)(PPhMe_2)]$ and $[MnBr_2(O_2)(PPhMe_2)]$, from which it can be seen that similar visible spectral profiles are exhibited, although the band maxima occur at different energies. We earlier pointed out the similar ligating abilities of isocyanide and phosphine ligands, and can only reiterate that we are puzzled by the fact that $[MnBr_2(CNBu^t)(PPhMe_2)]$ is deep blue in colour whilst $[MnBr_2(PPhMe_2)_2]$ is colourless.[33]

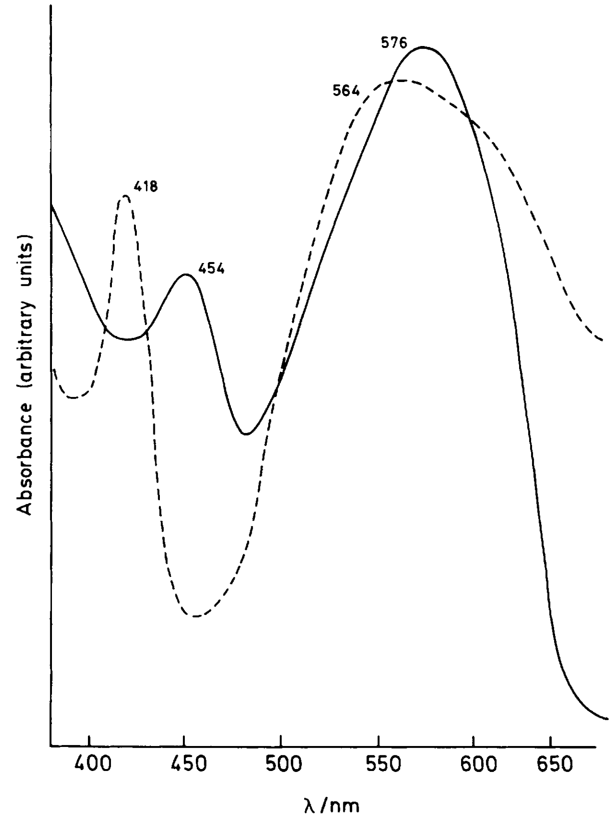

Figure 1. Solid visible reflectance spectra of $[\mathrm{MnBr_2(CNBu^t)(PPhMe_2)}]$ (——) and $[\mathrm{MnBr_2(O_2)(PPhMe_2)}]$ (- - - -)

A red solution forms when $[\mathrm{MnBr_2(CNBu^t)(PPhMe_2)}]$ is dissolved in ethanol. A rearrangement occurs very quickly; immediate addition of toluene to this red solution causes precipitation of $[\mathrm{Mn(CNBu^t)_4(PPhMe_2)_2}][\mathrm{MnBr_4}]$ (Scheme, Table 1). The anion $[\mathrm{MnBr_4}]^{2-}$ can be replaced by $2[\mathrm{PF_6}]^-$ by addition of $\mathrm{NH_4PF_6}$ to the red ethanolic solution. Replacement of the phosphine ligand in $[\mathrm{MnBr_2(CNBu^t)(PPhMe_2)}]$ by $\mathrm{PPr^n{}_3}$, $\mathrm{PPhEt_2}$, or $\mathrm{PPh_2Me}$ can lead subsequently to the isolation of other $[\mathrm{Mn(CNBu^t)_4(PR_3)_2}][\mathrm{PF_6}]_2$ species ($\mathrm{PR_3}$ = $\mathrm{PPh_2Me}$, $\mathrm{PPhEt_2}$, or $\mathrm{PPr^n{}_3}$ (Table 1).

All the $[\mathrm{Mn(CNBu^t)_4(PR_3)_2}]^{2+}$ complexes exhibit single i.r. bands in the region 2 138—2 142 $\mathrm{cm^{-1}}$, assignable to ν(CN) (Table 1). Again, as in $[\mathrm{MnBr_2(CNBu^t)(PPhMe_2)}]$, the bands are shifted to higher frequency when compared to ν(CN) in free $\mathrm{CNBu^t}$, 2 122 $\mathrm{cm^{-1}}$. The occurrence of a single ν(CN) absorption is consistent with the four isocyanides being in equivalent equatorial positions. All the complexes also exhibit ν(Mn–C) in the range 310—315 $\mathrm{cm^{-1}}$. The $[\mathrm{Mn(CNBu^t)_4(PR_3)_2}][\mathrm{PF_6}]_2$ complexes also exhibit bands assignable to ν(P–F) between 838 and 842 $\mathrm{cm^{-1}}$, similar to bands reported for $[\mathrm{Cr(CNR)_4(PR'_3)_2}][\mathrm{PF_6}]_2$ complexes.[10] A band assignable to terminal ν(Mn–Br) is exhibited by $[\mathrm{Mn(CNBu^t)_4(PPhMe_2)_2}][\mathrm{MnBr_4}]$ (Table 1).

The $[\mathrm{Mn(CNBu^t)_4(PR_3)_2}]^{2+}$ cation is low-spin, a value of 2.2 μ_B being obtained for $[\mathrm{Mn(CNBu^t)_4(PPhMe_2)_2}][\mathrm{PF_6}]_2$ at room temperature. No absorptions in the room-temperature X-band e.s.r. spectrum are observed for the complexes $[\mathrm{Mn(CNBu^t)_4(PR_3)_2}][\mathrm{PF_6}]_2$, consistent with the observed low-spin configuration; spectra are only expected close to liquid helium temperatures.[39] The X-band powder e.s.r. spectrum of $[\mathrm{Mn(CNBu^t)_4(PPhMe_2)_2}][\mathrm{MnBr_4}]$ exhibits an intense signal at g = 2 and a very weak signal at g = 4, the spectrum being identical to that of $[\mathrm{PPh_3(cyclo\text{-}C_6H_{11})}]_2[\mathrm{MnBr_4}]$. The X-band e.s.r. spectrum of an ethanol glass of $[\mathrm{Mn(CNBu^t)_4(PPhMe_2)_2}][\mathrm{MnBr_4}]$ at 93 K shows complex absorptions in the range 500—4 500 G (Figure 2). The spectrum is identical to that of an ethanol glass of $[\mathrm{PPh_3(cyclo\text{-}C_6H_{11})}]_2[\mathrm{MnBr_4}]$ at 93 K (Figure 2); the absorption at g = 6 is characteristic of a degree of axial symmetry, suggesting that the species **(III)** is present.

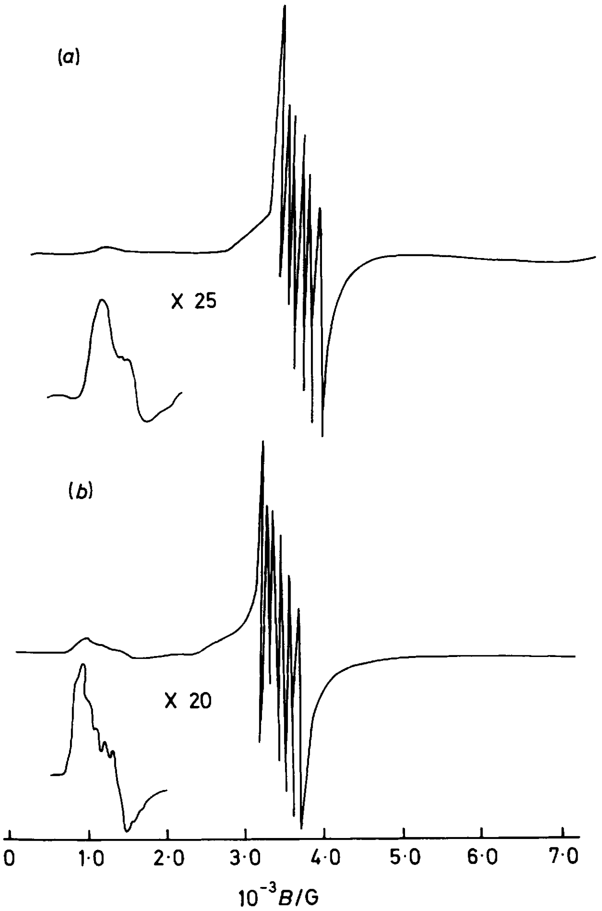

Figure 2. E.s.r. spectra of (*a*) $[\mathrm{Mn(CNBu^t)_4(PPhMe_2)_2}][\mathrm{MnBr_4}]$ and (*b*) $[\mathrm{PPh_3(cyclo\text{-}C_6H_{11})}]_2[\mathrm{MnBr_4}]$ in ethanol glasses at 93 K

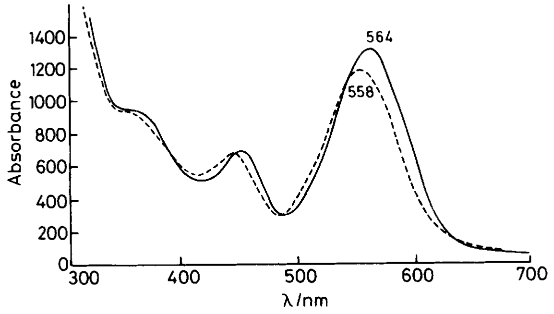

Figure 3. Visible spectra of $[\mathrm{Mn(CNBu^t)_4(PPhMe_2)_2}][\mathrm{MnBr_4}]$ (- - - -) and $[\mathrm{Mn(CNBu^t)_4(PPhMe_2)_2}][\mathrm{PF_6}]_2$ (——) in solution

The visible solution spectra of $[\mathrm{Mn(CNBu^t)_4(PPhMe_2)_2}][\mathrm{MnBr_4}]$ and $[\mathrm{Mn(CNBu^t)_4(PPhMe_2)_2}][\mathrm{PF_6}]_2$ are shown in Figure 3, and the main band maxima are at 558 and 564 nm, respectively. The close proximity of the values suggests that the cation $[\mathrm{Mn(CNBu^t)_4(PPhMe_2)_2}]^{2+}$ is responsible for the colour. Because of solubility differences the spectra were

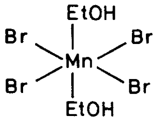

(III)

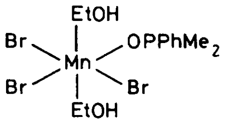

(IV)

obtained in different solvents and this may account for the slight differences in band maxima energies.

When the red ethanolic solution of $[Mn(CNBu^t)_4(PPhMe_2)_2][MnBr_4]$ was allowed to stand in air for a period of days small red crystals of $[Mn(CNBu^t)_4(PPhMe_2)_2][MnBr_3(OPPhMe_2)]_2$, suitable for *X*-ray analysis were obtained (see below). The monomeric pseudo octahedral structure of the cation is similar to that postulated by Walton and co-workers[10] for the $[Cr(CNR)_4(PR'_3)_2]^{2+}$ cations. The $[MnBr_3(OPPhMe_2)]^-$ anion, ν(P=O) 1 148 cm^{-1} and ν(Mn–Br) 226 cm^{-1}, is presumably formed by the dissociation of $PPhMe_2$ from $[Mn(CNBu^t)_4(PPhMe_2)_2]^{2+}$ and its subsequent oxidation by air. It is possible to prepare the complex $[PPh_3(cyclo\text{-}C_6H_{11})][MnBr_3(OPPhMe_2)]$ by mixing stoicheiometric quantities of $[PPh_3(cyclo\text{-}C_6H_{11})]_2[MnBr_4]$ and $OPPhMe_2$ in ethanol, and this complex also exhibits ν(P=O) at 1 148 cm^{-1} and terminal ν(Mn–Br) at 226 cm^{-1}. The *X*-band e.s.r. spectrum of an ethanol glass of $[PPh_3(cyclo\text{-}C_6H_{11})][MnBr_3(OPPhMe_2)]$ is similar to that of an ethanol glass of $[PPh_3(cyclo\text{-}C_6H_{11})]_2[MnBr_4]$ (Figure 2) strongly suggesting that co-ordination of ethanol occurs in solution to yield a structure, (**IV**), similar to that proposed above for $[MnBr_4]^{2-}$ in ethanol, (**III**).

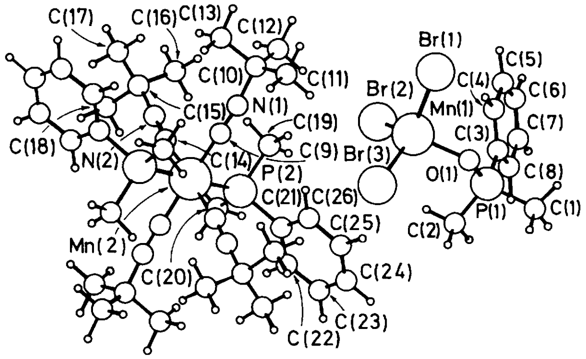

Figure 4. Molecular structure of $[Mn(CNBu^t)_4(PPhMe_2)_2][MnBr_3(OPPhMe_2)]_2$ showing atom labelling scheme. Drawn using PLUTO[43]

Crystal Structure of $[Mn(CNBu^t)_4(PPhMe_2)_2][MnBr_3(OPPhMe_2)]_2$.—The crystal comprises $[Mn(CNBu^t)_4(PPhMe_2)_2]^{2+}$ cations in which the octahedrally co-ordinated manganese lies on a crystallographic inversion centre. $[MnBr_3(OPPhMe_2)]^-$ anions complete the structure. The molecular ions, including the atom labelling scheme, are shown in Figure 4 with fractional atomic co-ordinates and bond lengths and angles presented in Tables 2 and 3. The $PPhMe_2$ ligand dimensions are unremarkable, resembling those in $[MnI_2(PPhMe_2)]$.[32] However, the Mn–P bond at 2.344(3) Å is

Table 2. Fractional atomic co-ordinates (× 10^4) for non-hydrogen atoms of the complex $[Mn(CNBu^t)_4(PPhMe_2)_2][MnBr_3(OPPhMe_2)]_2$

Atom	*X*/*a*	*Y*/*b*	*Z*/*c*
Mn(1)	3 250(1)	3 525(1)	10 487(2)
Br(1)	4 336(1)	3 815(1)	12 572(1)
Br(2)	4 047(1)	3 838(1)	8 660(1)
Br(3)	968(1)	3 519(1)	10 187(2)
P(1)	4 138(2)	2 508(1)	9 745(3)
O(1)	3 800(6)	2 867(2)	10 610(7)
C(1)	4 128(9)	1 961(3)	10 430(11)
C(2)	3 119(8)	2 496(4)	8 290(12)
C(3)	5 668(8)	2 605(3)	9 464(11)
C(4)	6 395(9)	2 935(3)	10 157(13)
C(5)	7 577(9)	3 014(3)	9 976(14)
C(6)	8 030(9)	2 764(4)	9 064(14)
C(7)	7 313(9)	2 443(4)	8 391(14)
C(8)	6 105(9)	2 361(3)	8 551(13)
Mn(2)	0	5 000	5 000
P(2)	1 316(2)	4 446(1)	4 449(3)
N(1)	1 744(7)	5 154(3)	7 521(10)
N(2)	1 723(6)	5 677(3)	4 060(9)
C(9)	1 075(7)	5 089(3)	6 592(10)
C(10)	2 638(10)	5 289(4)	8 666(14)
C(11)	2 377(16)	5 015(6)	9 778(16)
C(12)	3 929(9)	5 180(4)	8 437(16)
C(13)	2 493(12)	5 800(4)	8 854(16)
C(14)	1 038(7)	5 436(3)	4 370(9)
C(15)	2 574(9)	5 988(4)	3 638(14)
C(16)	3 806(9)	5 755(5)	3 843(18)
C(17)	2 580(11)	6 419(4)	4 384(17)
C(18)	2 063(14)	6 077(6)	2 217(18)
C(19)	2 935(8)	4 501(4)	5 206(12)
C(20)	1 370(10)	4 469(4)	2 775(11)
C(21)	985(7)	3 868(3)	4 807(12)
C(22)	641(9)	3 543(4)	3 881(13)
C(23)	398(11)	3 106(5)	4 227(21)
C(24)	526(11)	2 981(5)	5 442(22)
C(25)	858(9)	3 294(4)	6 351(16)
C(26)	1 090(8)	3 739(4)	6 076(14)

Table 3. Selected bond lengths (Å) and angles (°)

Mn(1)–Br(1)	2.478(2)	P(2)–C(20)	1.81(1)	Mn(1)–Br(2)	2.485(2)	P(2)–C(21)	1.81(1)
Mn(1)–Br(3)	2.478(2)	N(1)–C(9)	1.14(1)	Mn(1)–O(1)	2.035(6)	N(1)–C(10)	1.47(2)
P(1)–O(1)	1.505(8)	N(2)–C(14)	1.14(1)	P(1)–C(1)	1.78(1)	N(2)–C(15)	1.45(1)
P(1)–C(2)	1.74(1)	C(10)–C(11)	1.52(2)	P(1)–C(3)	1.80(1)	C(10)–C(12)	1.53(2)
C(3)–C(4)	1.38(1)	C(10)–C(13)	1.54(2)	C(3)–C(8)	1.38(2)	C(15)–C(16)	1.50(2)
C(4)–C(5)	1.38(2)	C(15)–C(17)	1.50(2)	C(5)–C(6)	1.40(2)	C(15)–C(18)	1.54(2)
C(5)–C(7)	1.35(2)	C(21)–C(22)	1.38(2)	C(7)–C(8)	1.40(2)	C(21)–C(26)	1.40(2)
Mn(2)–P(2)	2.344(3)	C(22)–C(23)	1.38(2)	Mn(2)–C(9)	1.898(9)	C(23)–C(24)	1.34(3)
Mn(2)–C(14)	1.935(9)	C(24)–C(25)	1.34(2)	P(2)–C(19)	1.82(1)	C(25)–C(26)	1.39(2)
Br(2)–Mn(1)–Br(1)	113.6(1)	C(14)–Mn(2)–P(2)	86.4(3)	Br(3)–Mn(1)–Br(1)	114.7(1)	C(9)–Mn(2)–P(2)	90.9(3)
Br(3)–Mn(1)–Br(2)	114.2(1)	C(19)–P(2)–Mn(2)	115.3(4)	O(1)–Mn(1)–Br(1)	100.8(2)	C(14)–Mn(2)–C(9)	85.1(4)
O(1)–Mn(1)–Br(2)	105.1(2)	C(20)–P(2)–Mn(2)	111.5(4)	O(1)–Mn(1)–Br(3)	106.6(2)	C(20)–P(2)–C(19)	102.6(5)
C(1)–P(1)–O(1)	111.3(5)	C(21)–P(2)–Mn(2)	116.5(4)	C(2)–P(1)–O(1)	112.0(5)	C(21)–P(2)–C(19)	102.3(5)
C(2)–P(1)–C(1)	107.3(5)	C(21)–P(2)–C(20)	107.2(6)	C(3)–P(1)–O(1)	110.3(4)	N(1)–C(9)–Mn(2)	177.2(9)
C(3)–P(1)–C(1)	107.3(4)	N(2)–C(14)–Mn(2)	174.7(7)	C(3)–P(1)–C(2)	108.4(5)		
P(1)–O(1)–Mn(1)	137.8(5)						

substantially shorter than the corresponding distances in the iodo complex, average 2.671 Å. The $CNBu^t$ dimensions compare well with those reported for $[Mn(CO)_2(CNBu^t)(CNPh)(phen)]ClO_4$(phen = 1,10-phenanthroline)[40] as do the Mn–C bond lengths. The anion dimensions are as expected with bond lengths and angles falling within the expected range.

Experimental

All manipulations involving air-sensitive materials were performed under a dry argon atmosphere, and solvents and manganese(II) salts were dried by published procedures.[41] t-Butyl isocyanide was obtained from the Fluka Chemical Co.

Preparations.—$[MnBr_2(CNBu^t)(PPhMe_2)]$. This complex can be prepared by two methods: (*a*) to toluene (50 cm^3), in a flame-dried 250-cm^3 side-arm flask, was added $[MnBr_2(PPhMe_2)]$ (0.50 g, 1.41 mmol). t-Butyl isocyanide (0.16 cm^3, 1.41 mmol) was added and the mixture stirred for *ca.* 48 h. The resulting deep blue-purple complex was filtered using a Schlenk apparatus, washed with dry toluene (3 × 50 cm^3), and dried *in vacuo* at 40 °C; (*b*) to $MnBr_2$ (0.40 g, 1.86 mmol) in dry toluene (50 cm^3) was added $PPhMe_2$ (0.27 cm^3, 1.86 mmol) followed by $CNBu^t$ (1.86 mmol); the mixture was stirred for 48 h with work-up as in (*a*).

trans-$[Mn(CNBu^t)_4(PPhMe_2)_2][MnBr_4]$. The blue-purple complex $[MnBr_2(CNBu^t)(PPhMe_2)]$ (0.60 g, 1.37 mmol) was dissolved in ethanol (30 cm^3) to give a red solution, and immediately toluene (40 cm^3) was added to give a red, finely divided precipitate. This was filtered off to yield a red air-stable complex.

trans-$[Mn(CNBu^t)_4(PPhMe_2)_2][MnBr_3(OPPhMe_2)]_2$. The method of preparation was essentially the same as for *trans*-$[Mn(CNBu^t)_4(PPhMe_2)_2][MnBr_4]$. However, instead of precipitation of the complex with toluene, the ethanol solvent was allowed to slowly evaporate, producing large red crystals, which were filtered off, dried in air, and one was found to be suitable for *X*-ray analysis.

trans-$[Mn(CNBu^t)_4(PPhMe_2)_2][PF_6]_2$. The red complex *trans*-$[Mn(CNBu^t)_4(PPhMe_2)_2][MnBr_4]$ (0.40 g, 0.39 mmol) was dissolved in ethanol (30 cm^3). Excess NH_4PF_6 (Fluorochem Ltd.) was added and the solution cooled in an ice-bath. The resulting red-pink precipitate was filtered off and dried in air.

$[PPh_3(cyclo\text{-}C_6H_{11})][MnBr_3(OPPhMe_2)]$. To an ethanolic solution (20 cm^3) of $[PPh_3(cyclo\text{-}C_6H_{11})]_2[MnBr_4]$ (0.20 g, 0.19 mmol) was added $OPPhMe_2$ (0.03 g, 0.19 mmol) dissolved in ethanol (10 cm^3), and the solvent was allowed to evaporate slowly at 35 °C. The resulting green-yellow crystals of $[PPh_3(cyclo\text{-}C_6H_{11})][MnBr_3(OPPhMe_2)]$ were dried in air.

Crystal Structure Determination.—*Crystal data.* $C_{52}H_{80}Br_6Mn_3N_4O_2P_4$, M = 1 561.47, monoclinic, space group $P2_1/c$, a = 11.050(1), b = 29.579(5), c = 10.745(1) Å, β = 101.40(3)°, U = 3 442(1) Å^3, Z = 2, D_c = 1.41 Mg m^{-3}, μ(Mo-K_α) = 4.04 mm^{-1}, T = 293 K, F(000) = 1 550. A red crystal of $[Mn(CNBu^t)_4(PPhMe_2)_2][MnBr_3(OPPhMe_2)]_2$, 0.2 × 0.3 × 0.3 mm, was sealed in a Lindemann tube. Diffraction data were collected on an Enraf–Nonius CAD4 diffractometer using Mo-K_α radiation and ω–2θ scan mode. 3 435 Reflections were measured ($I > 0$, $1 < \theta < 25°$, $\pm h$, $\pm k$, $\pm l$) resulting in 3 195 unique $F > 3\sigma(F)$. Negligible fluctuation was observed in three intensity standards measured repeatedly at 3 h intervals. Lorentz-polarisation corrections were applied but absorption ignored. Cell parameters were calculated by least-squares refinement on setting angles of 25 accurately centred reflections.

Normal heavy-atom techniques were used to solve the structure. Blocked-matrix least-squares refinement using SHELX[42] with all non-hydrogen atoms treated anisotropically and all hydrogen atoms constrained to chemically reasonable positions[43] with shared isotropic parameters, common to each molecule, gave R = 0.070, R' = 0.076 [$w = 1/\sigma^2(F_o)$]. The highest feature in the final difference Fourier map is a peak of 0.83 e Å^{-3} located near Br(1); there is also a relatively high vibrational parameter for Br(3) [U_{22} = 0.140(1) Å^2]. These observations suggest that the anion is slightly disordered, which is the probable cause of the slightly elevated R factor. All calculations were performed on the joint CDC 7600/Amdahl 470 system of the University of Manchester Regional Computing Centre.

Additional material available from the Cambridge Crystallographic Data Centre comprises thermal parameters, H-atom co-ordinates, remaining bond lengths and angles, and torsion angles.

References

1 L. Malatest and F. Bonati, 'Isocyanide Complexes of Metals,' J. Wiley Inc., New York, 1971.
2 Y. Yamamoto, *Coord. Chem. Rev.*, 1980, **32**, 95.
3 P. Brant, F. A. Cotton, J. C. Sekutowski, T. E. Wood, and R. A. Walton, *J. Am. Chem. Soc.*, 1979, **101**, 6588.
4 W. S. Mialki, T. E. Wood, and R. A. Walton, *J. Am. Chem. Soc.*, 1980, **102**, 7105.
5 J. C. Dewan, W. S. Mialki, R. A. Walton, and S. J. Lippard, *J. Am. Chem. Soc.*, 1982, **104**, 133.
6 J. A. Connor and C. Overton, *J. Chem. Soc., Dalton Trans.*, 1982, 2397.
7 K. R. Mann, M. Cimilino, G. L. Geoffry, G. S. Hammond, A. A. Orio, G. Albertin, and H. B. Gray, *Inorg. Chim. Acta*, 1976, **16**, 97.
8 P. Fantucci, L. Naldini, F. Cariati, V. Valenti, and C. J. Bussetto, *J. Organomet. Chem.*, 1974, **64**, 109.
9 D. D. Klendworth, W. W. Welters, and R. A. Walton, *Organometallics* 1982, **1**, 336.
10 W. S. Mialki, D. E. Wigley, T. E. Wood, and R. A. Walton, *Inorg. Chem.*, 1982, **21**, 480.
11 D. E. Wigley and R. A. Walton, *Organometallics*, 1982, **1**, 1322.
12 J. L. Pierce, D. E. Wigley, and R. A. Walton, *Organometallics*, 1982, **1**, 1328.
13 J. D. Allison, T. E. Wood, R. E. Wilde, and R. A. Walton, *Inorg. Chem.*, 1982, **21**, 480.
14 D. A. Bohling, J. F. Evans, and K. R. Mann, *Inorg. Chem.*, 1982, **21**, 3546.
15 K. R. Mann, G. S. Hammond, and H. B. Gray, *J. Am. Chem. Soc.*, 1977, **99**, 309.
16 M. J. Abrams, A. Davison, J. W. Brodack, A. G. Jones, R. Faggiani, and L. J. C. Lock, *J. Labelled Compd. Radiopharm.*, 1982, **14**, 1596.
17 M. J. Abrams, A. Davison, A. G. Jones, C. E. Costello, and H. Pang, *Inorg. Chem.*, 1983, **22**, 2798.
18 P. M. Treichel and G. E. Dirreen, *J. Organomet. Chem.*, 1972, **39**, C20.
19 D. T. Plummer and R. J. Angelici, *Inorg. Chem.*, 1983, **22**, 4063.
20 P. M. Treichel, G. E. Dirreen, and H. J. Mueh, *J. Organomet. Chem.*, 1972, **44**, 339.
21 P. M. Treichel, D. W. Firsich, and G. P. Essenmacher, *Inorg. Chem.*, 1979, **18**, 2405 and refs. therein.
22 L. Naldini, *Gazz. Chim. Ital.*, 1960, **90**, 871.
23 D. S. Matteson and R. A. Bailey, *J. Am. Chem. Soc.*, 1968, **90**, 3761.
24 F. A. Cotton and F. Zingales, *J. Am. Chem. Soc.*, 1961, **83**, 351.
25 C. A. McAuliffe, H. Al-Khateeb, D. S. Barratt, J. C. Briggs, A. Chalitta, A. Hosseiny, M. G. Little, A. G. Mackie, and K. Minten, *J. Chem. Soc., Dalton Trans.*, 1983, 2147.
26 D. S. Barratt, G. A. Grott, and C. A. McAuliffe, *J. Chem. Soc., Dalton Trans.*, 1988, 2065.
27 C. G. Benson, C. A. McAuliffe, A. G. Mackie, and S. P. Tanner, *Inorg. Chim. Acta*, 1987, **128**, 191.
28 C. A. McAuliffe, D. S. Barratt, C. G. Benson, A. Hosseiny, M. G. Little, and K. Minten, *J. Organomet. Chem.*, 1983, **258**, 35.
29 D. S. Barratt and C. A. McAuliffe, *J. Chem. Soc., Chem. Commun.*, 1984, 594.

30 D. S. Barratt, C. G. Benson, G. A. Gott, C. A. McAuliffe, and S. P. Tanner, *J. Chem. Soc., Dalton Trans.*, 1985, 2661.
31 D. S. Barratt and C. A. McAuliffe, *Inorg. Chim. Acta*, 1985, **97**, 37.
32 T. J. King, B. Beagley, J. C. Briggs, A. Hosseiny, C. A. McAuliffe, K. Minten, and W. E. Hill, *J. Chem. Soc., Chem. Commun.*, 1984, 305.
33 J. C. Briggs, A. Challita, B. Beagley, C. A. McAuliffe, and R. G. Pritchard, unpublished work.
34 C. G. Howard, G. S. Girolami, G. Wilkinson, M. Thornton-Pett, and M. B. Hursthouse, *J. Chem. Soc., Dalton Trans.*, 1983, 2631.
35 N. Hebendanz, F. H. Kohler, and G. Muller, *Inorg. Chem.*, 1984, **23**, 3044.
36 F. Bonati and G. Minghetti, *Inorg. Chim. Acta*, 1974, **9**, 95.
37 F. A. Cotton and R. V. Parish, *J. Chem. Soc.*, 1960, 1440.
38 G. A. Gott and C. A. McAuliffe, *J. Chem. Soc., Dalton Trans.*, 1987, 1785.
39 J. F. Gibson, 'ESR and NMR of Paramagnetic Species in Biological and Related Systems,' NATO Advanced Study Institute Series, eds. I. Bertini and R. S. Drago, D. Reidel Publishing Co., Dordrecht, 1979 and refs. therein.
40 M. L. Valin, D. Moreiras, X. Solans, M. Font-Altaba, J. Solans, F. J. Garcia-Alonso, V. Riera, and M. Viranco, *Acta Crystallogr., Sect. C*, 1985, **41**, 1312.
41 A. Hosseiny, C. A. McAuliffe, A. G. Mackie, and K. Minten, *Inorg. Chim. Acta*, 1981, **49**, 99.
42 G. M. Sheldrick, SHELX 76, Program for crystal structure determination, University of Cambridge, 1976.
43 W. D. S. Motherwell and W. Clegg, PLUTO, Program for plotting molecular and crystal structures, University of Cambridge, 1978.

Received 29th July 1987; *Paper* 7/1384